THE SPHERICAL HARMONICS ROOT-MUSIC

Lalan Kumar, Guoan Bi

School of EEE
Nanyang Technological University, Singapore
Email : {lkumar,egbi}@ntu.edu.sg

Rajesh M. Hegde

Electrical Engineering Dept.
Indian Institute of Technology, Kanpur
Email : rhegde@iitk.ac.in

ABSTRACT

Spherical harmonics root-MUSIC (MUltiple SIgnal Classification) technique for source localization using spherical microphone array is presented in this paper. Earlier work on root-MUSIC is limited to linear and planar arrays. Root-MUSIC for planar array utilizes the concept of manifold separation and beamspace transformation. In this paper, the Vandermonde structure of array manifold for a particular order is proved. Hence, the validity of root-MUSIC in the spherical harmonics domain is confirmed. The proposed method is evaluated by using simulated experiments on source localization. Root mean square error analysis and statistical analysis are presented. The experimental measures at various signal to noise ratios (SNRs) show the robustness of the proposed method. The method is also verified by using experiment on real signal acquired over spherical microphone array.

***Index Terms*—** Root-MUSIC, Spherical microphone array, Spherical harmonics, Manifold separation

1. INTRODUCTION

The use of accurate and search free algorithms for estimating direction of arrival (DOA) has been a very active research area in source localization. Root-MUSIC (MUltiple SIgnal Classification) [1] and Estimation of Signal Parameters using Rotational Invariance Techniques, ESPRIT [2], fall into this category. The root-MUSIC method estimates DOAs as the roots of MUSIC [3] polynomial owing to Vandermonde structure of array manifold. Such a structure is not observed in array manifold for uniform circular array (UCA) [4]. Zoltowski proposed beamspace transformation based on phase mode excitation to get the Vandermonde structure in array manifold with respect to azimuth angle [5]. Hence, it enables the application of root-MUSIC to azimuth estimation at a given elevation. The technique was further extended to sparse UCA root-MUSIC in order to utilize the modified beamspace transformation [6]. Another approach for extending the ULA root-MUSIC to a planar array is presented in [7] using manifold separation. The idea of manifold separation is to write the planar array steering vector (array manifold) as a product of a characteristic matrix of the array and a vector with Vandermonde structure depending on the azimuth angle. The manifold separation which utilizes spherical harmonics (SH) is introduced in [8].

After the introduction of higher order spherical microphone array and associated signal processing in [9] and [10], various existing DOA estimation techniques were reformulated in the spherical harmonics domain. The element space MUSIC was implemented in terms of spherical harmonics, called SH-MUSIC, in [11] and [12]. The Minimum Variance Distortionless Response (MVDR) spectrum in terms of spherical harmonics, SH-MVDR, was utilized for DOA estimation in [11]. MUSIC-Group delay [13] was formulated for source localization using spherical array in [14] and [15]. Differential geometry was explored for SH domain source localization in [16]. In this work, we have developed the theory of root-MUSIC in SH domain using manifold separation technique. The theory is validated using simulation and real data experiments. The proposed SH-root-MUSIC (SH-RM) technique provides exact solution without the limitation from the discretization issues associated with the SH-MUSIC and SH-MVDR methods for DOA estimation.

This work was funded in part by DST project EE/SERB/20130277 and in part by BITCOE, IIT Kanpur.

2. THE SPHERICAL HARMONICS DATA MODEL

A spherical microphone array of order N, radius r and the number of sensors I is considered. A sound field of L plane-waves is incident on the array with wavenumber k. The l^{th} source location is denoted by $\Psi_l = (\theta_l, \phi_l)$. The elevation angle θ is measured from the positive z axis, while the azimuthal angle ϕ is measured counterclockwise from the positive x axis. Similarly, the i^{th} sensor location is given by $\Phi_i = (\theta_i, \phi_i)$.

In spatial domain, the sound pressure at I microphones, $\mathbf{p}(k) = [p_1(k), p_2(k), \dots, p_I(k)]^T$, is written as

$$\mathbf{p}(k) = \mathbf{V}(k)\mathbf{s}(k) + \mathbf{n}(k) \tag{1}$$

where $p_i(k) \equiv p(k, r, \theta_i, \phi_i)$, $\mathbf{V}(k)$ is an $I \times L$ steering matrix, $\mathbf{s}(k)$ is a $L \times 1$ vector of signal amplitudes, $\mathbf{n}(k)$ is an $I \times 1$ vector of zero mean, uncorrelated sensor noise and $(.)^T$ denotes the transpose. The steering matrix $\mathbf{V}(k)$ is expressed as

$$\mathbf{V}(k) = [\mathbf{v_1}(k), \mathbf{v_2}(k), \dots, \mathbf{v_L}(k)], \text{ where} \tag{2}$$

$$\mathbf{v}_l(k) = [e^{-j\mathbf{k}_l^T\mathbf{r}_1}, e^{-j\mathbf{k}_l^T\mathbf{r}_2}, \dots, e^{-j\mathbf{k}_l^T\mathbf{r}_I}]^T \tag{3}$$

$$\mathbf{k}_l = -(k\sin\theta_l\cos\phi_l, k\sin\theta_l\sin\phi_l, k\cos\theta_l)^T \tag{4}$$

$$\mathbf{r}_i = (r\sin\theta_i\cos\phi_i, r\sin\theta_i\sin\phi_i, r\cos\theta_i)^T \tag{5}$$

where $j = \sqrt{-1}$. The i^{th} term in (3) refers to the pressure due to l^{th} unit amplitude planewave with wavevector $\mathbf{k}_l$ at location $\mathbf{r}_i$. This may alternatively be written as [17]

$$e^{-j\mathbf{k}_l^T\mathbf{r}_i} = \sum_{n=0}^{\infty}\sum_{m=-n}^{n} b_n(kr)[Y_n^m(\Psi_l)]^* Y_n^m(\Phi_i) \tag{6}$$

where $b_n(kr)$ is called mode strength.

The far-field mode strength, $b_n(kr)$, is given by

$$b_n(kr) = 4\pi j^n j_n(kr), \quad \text{for open sphere} \tag{7}$$

$$= 4\pi j^n \big(j_n(kr) - \frac{j_n'(kr)}{h_n'(kr)}\big), \quad \text{for rigid sphere} \tag{8}$$

where $j_n(kr)$ is the spherical Bessel function, $h_n(kr)$ is n^{th} order spherical Hankel function of second kind and $'$ refers to the first derivative. Figure 1 illustrates mode strength b_n as a function of kr and n for an open sphere. For $kr = 0.1$, the zeroth order mode amplitude is 22 dB, while the first order has an amplitude of -8 dB. It is seen that for an order greater than kr, the mode strength b_n decreases significantly. Therefore, the summation in (6) is truncated to a finite value of N, which is known as the array order.

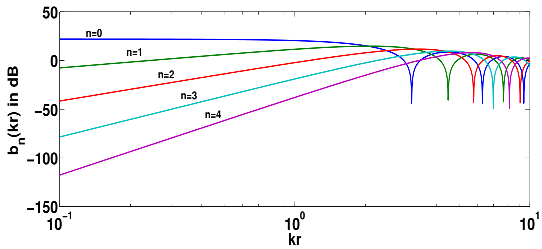

Fig. 1. Mode amplitude b_n for an open sphere as a function of kr and n

The spherical harmonic of order n and degree m, $Y_n^m(\Psi)$, is given by

$$\begin{aligned} Y_n^m(\Psi) &= \sqrt{\frac{(2n+1)(n-m)!}{4\pi(n+m)!}} P_n^m(cos\theta)e^{jm\phi}, \\ &\forall 0 \leq n \leq N, 0 \leq m \leq n \\ &= (-1)^{|m|} Y_n^{|m|*}(\Psi), \forall -n \leq m < 0, \end{aligned} \tag{9}$$

where Y_n^m is solution to the Helmholtz equation [18] and P_n^m is the associated Legendre function. Figure 2 shows the plot of three spherical harmonics. It should be noted that Y_0^0 is isotropic while Y_1^0 and Y_1^1 have directional characteristics. The spherical harmonics are used for spherical harmonics decomposition of a square integrable function, similar to the complex exponential $e^{j\omega t}$ used for decomposition of real periodic functions [19].

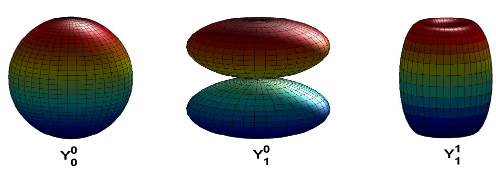

Fig. 2. Spherical harmonics plot, Y_0^0, Y_1^0, Y_1^1

Substituting (3) and (6) in (2), the expression of steering matrix becomes

$$\mathbf{V}(k) = \mathbf{Y}(\Phi)\mathbf{B}(kr)\mathbf{Y}^H(\Psi) \tag{10}$$

where $\mathbf{Y}(\Phi)$ is $I \times (N+1)^2$ matrix whose i^{th} row is given as

$$\mathbf{y}(\Phi_i) = [Y_0^0(\Phi_i), Y_1^{-1}(\Phi_i), Y_1^0(\Phi_i), Y_1^1(\Phi_i), \ldots, Y_N^N(\Phi_i)]. \tag{11}$$

The $L \times (N+1)^2$ matrix $\mathbf{Y}(\Psi)$ can be expanded on similar lines. The $(N+1)^2 \times (N+1)^2$ matrix $\mathbf{B}(kr)$ is given by

$$\mathbf{B}(kr) = diag(b_0(kr), b_1(kr), b_1(kr), b_1(kr), \ldots, b_N(kr)). \tag{12}$$

With the introduction of spherical harmonics, the spherical harmonics decomposition of the received pressure, $p(k)$, is given as [20]

$$\begin{aligned} p_{nm}(k) &= \int_0^{2\pi}\int_0^{\pi} p(k)[Y_n^m(\Phi)]^* \sin(\theta) d\theta d\phi \\ &\cong \sum_{i=1}^{I} a_i p_i(k)[Y_{nm}(\Phi_i)]^*, \end{aligned} \tag{13}$$

where $p_{nm}(k)$ is spherical Fourier coefficient. The spatial sampling of pressure over a spherical microphone array is captured by using sampling weights, a_i [21]. Re-writing (13) in a matrix form, we have

$$\mathbf{p_{nm}}(k) = \mathbf{Y}^H(\mathbf{\Phi})\mathbf{\Gamma}\mathbf{p}(k), \tag{14}$$

where $\mathbf{p_{nm}}(k) = [p_{00}, p_{1(-1)}, p_{10}, p_{11}, \ldots, p_{NN}]^T$ and $\mathbf{\Gamma} = \text{diag}(a_1, a_2, \cdots, a_I)$. Also, under the assumption of (13), we have the orthogonality property of spherical harmonics as follows

$$\mathbf{Y}^H(\mathbf{\Phi})\mathbf{\Gamma}\mathbf{Y}(\mathbf{\Phi}) = \mathbf{I}, \tag{15}$$

where $\mathbf{I}$ is an $(N+1)^2 \times (N+1)^2$ identity matrix. Substituting (10) in (1), then multiplying both sides with $\mathbf{Y}^H(\mathbf{\Phi})\mathbf{\Gamma}$ and utilizing the relations in (14) and (15), we have the data model in spherical harmonics domain as

$$\mathbf{p_{nm}}(k) = \mathbf{B}(kr)\mathbf{Y}^H(\Psi)\mathbf{s}(k) + \mathbf{n_{nm}}(k). \tag{16}$$

For a given array configuration, $\mathbf{B}(kr)$ is a constant. Therefore, we get the final spherical harmonics data model by multiplying both sides of (16) with $\mathbf{B}^{-1}(kr)$ as

$$\mathbf{a_{nm}}(k) = \mathbf{Y}^H(\Psi)\mathbf{s}(k) + \mathbf{z_{nm}}(k), \tag{17}$$

where

$$\mathbf{z_{nm}}(k) = \mathbf{B}^{-1}(kr)\mathbf{n_{nm}}(k). \tag{18}$$

3. THE SPHERICAL HARMONICS ROOT-MUSIC

Root-MUSIC estimates DOAs as roots of the MUSIC polynomial. Hence, we first write the MUSIC spectrum in spherical harmonics domain. Comparing the spatial data model in (1) with spherical harmonics data model in (17), $[\mathbf{Y}^H(\Psi)]_{(N+1)^2 \times L}$ is the steering matrix in spherical harmonics domain. Hence, the SH-MUSIC spectrum is written as

$$P_{SH-MUSIC}(\Psi) = \frac{1}{\mathbf{y}(\Psi)\mathbf{S}^{\mathbf{NS}}_{\mathbf{a_{nm}}}[\mathbf{S}^{\mathbf{NS}}_{\mathbf{a_{nm}}}]^H\mathbf{y}^H(\Psi)}, \tag{19}$$

where $\mathbf{y}^H(\Psi)$ is a steering vector defined in (11). $\mathbf{S}^{\mathbf{NS}}_{\mathbf{a_{nm}}}$ is the noise subspace obtained from eigenvalue decomposition of autocorrelation matrix, $\mathbf{S_{a_{nm}}} = E[\mathbf{a_{nm}}(k)\mathbf{a_{nm}}(k)^H]$. Frequency smoothing and whitening of noise should be applied as in [11]. The SH-MUSIC spectrum is shown in Figure 3(a) for two sources at (20°,40°) and (20°,80°). The two peaks in the figure correspond to the two sources.

The SH-MUSIC spectrum in (19) results in a peak which corresponds to a source owing to orthogonality between noise eigenvector and steering vector. A comprehensive search algorithm is needed to estimate the DOA of the desired source. The resolution is also limited by the resolution of discretization at which the spectrum is evaluated. The SH-root-MUSIC overcomes these limitations in estimating the DOAs. We first illustrate the Vandermonde structure in the steering vector using manifold separation technique. Utilizing

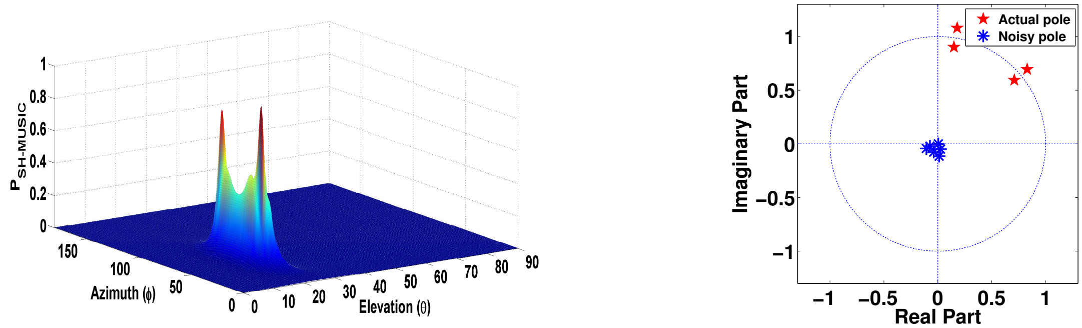

(a) (b)

Fig. 3. (a) SH-MUSIC spectrum (b) SH-root-MUSIC illustrating the actual DOA estimates (red poles) and noisy DOA estimates (blue poles) (order of the spherical array, $N = 4$, sources at (20°,40°), (20°,80°) and SNR=$15dB$).

(9) and (11), the steering vector for co-elevation θ_0 can be written in a more compact form as

$$\begin{aligned}\mathbf{y}^H(\Psi) &= \mathbf{y}^H(\theta_0, \phi) \\ &= [f_{00}, -f_{1(-1)}e^{j\phi}, f_{10}, f_{11}e^{-j\phi}, \cdots, f_{NN}e^{-jN\phi}]^T\end{aligned} \quad (20)$$

$$\text{where, } f_{nm} = \sqrt{\frac{(2n+1)(n-|m|)!}{4\pi(n+|m|)!}} P_n^{|m|}(cos\theta_0). \quad (21)$$

Then (20) is rewritten in a matrix form as

$$\mathbf{y}^H(\theta_0, \phi) = F(\theta_0)d(\phi) \quad (22)$$

$$\text{where, } F(\theta_0) = \text{diag}(f_{00}, -f_{1(-1)}, f_{10}, f_{11}, \cdots, f_{NN}) \quad (23)$$

$$d(\phi) = [1, e^{j\phi}, 1, e^{-j\phi}, \cdots, e^{-jN\phi}]^T. \quad (24)$$

The matrix $d(\phi)$ consists of only the exponent terms containing the azimuth angle and, each submatrix corresponding to a particular order follows the Vandermonde structure with common ratio as $e^{-j\phi}$. From (19) and (22), the SH-MUSIC cost function can be written as

$$\begin{aligned}P_{SHM}^{-1}(\phi) &= d^H(\phi)F^H(\theta_0)\mathbf{S}_{\mathbf{anm}}^{\mathbf{NS}}[\mathbf{S}_{\mathbf{anm}}^{\mathbf{NS}}]^H F(\theta_0)d(\phi) \\ &= d^H(\phi)F^H(\theta_0)\mathbf{C}F(\theta_0)d(\phi)\end{aligned} \quad (25)$$

$$\text{where } \mathbf{C} = \mathbf{S}_{\mathbf{anm}}^{\mathbf{NS}}[\mathbf{S}_{\mathbf{anm}}^{\mathbf{NS}}]^H.$$

By defining $z = e^{j\phi}$, the SH-MUSIC cost function now assumes a polynomial form of degree $4N$, given by

$$P_{SHM}^{-1}(\phi) = \sum_{u=-2N}^{2N} C_u z^u \quad (26)$$

where the coefficient C_u is obtained mathematically. The polynomial has $4N$ roots. If z is a root of the polynomial then $\frac{1}{z^*}$ will also be the root. Hence, $2N$ roots are within the unit circle while the other $2N$ roots are outside the unit circle. Of the $2N$ roots within the unit circle, L roots close to the unit circle correspond to the DOAs. This is illustrated in Figure 3(b) for a fourth order spherical microphone array. The roots are plotted for two sources with co-elevation angle 20° and azimuth angle (40°,80°) at SNR 15dB. All the roots within and near the unit circle are shown in the figure. The DOA can be estimated from the roots by using the relation, $\phi = \Im(ln(z))$, where $\Im()$ is the imaginary part of $()$.

4. PERFORMANCE EVALUATION

Simulation experiments based on source localization were carried out to evaluate the proposed SH-root-MUSIC method. Additionally, experiments were performed on real signal acquired over spherical microphone array to verify the algorithm. The experiments utilized an Eigenmike® system [22] which is shown in Figure 4. It consists of 32 microphones, embedded in rigid sphere of radius 4.2cm. The order of the microphone array was taken to be 4. Root mean square error (RMSE) and probability of resolution values were used to evaluate the source localization performance of the proposed method. The performance of the proposed method is compared to SH-MUSIC and SH-MVDR.

Fig. 4. The Eigenmike® setup in an anechoic chamber at IIT Kanpur for acquiring a far-field source.

4.1. Simulation Experiments on DOA Estimation

The RMSE analysis and statistical analysis are presented here for 500 independent Monte Carlo trials. The additive noise is assumed to be zero mean Gaussian distributed. Two sources with co-elevation 20° are considered.

4.1.1. RMSE Analysis

The experiments on source localization are presented as cumulative RMSE (CRMSE) computed by

$$CRMSE = \frac{1}{2T}\sum_{t=1}^{T}\sum_{l=1}^{2}[(\phi_l - \hat{\phi}_l^{(t)})^2], \quad (27)$$

where t is the trial index while l denotes the source index. The CRMSE values are plotted in Figure 5(a) with various SNR values

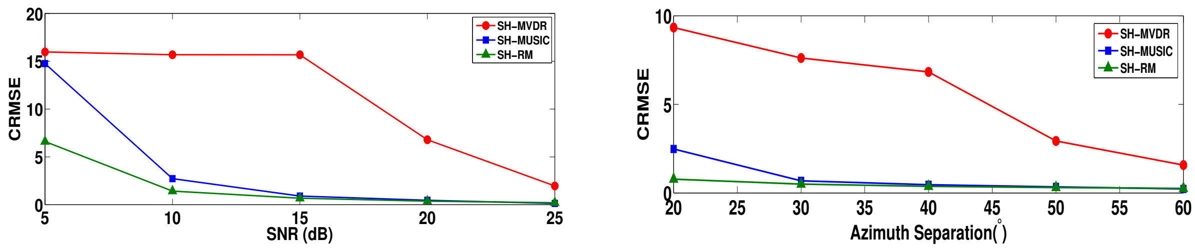

(a) (b)

Fig. 5. Cumulative RMSE for two sources with co-elevation 20°, (a) azimuth $(40^\circ, 80^\circ)$ at various SNRs. (b) azimuth of one source is fixed at 40° and that of other source is varying in steps of 10°. SNR$= 20dB$.

for two sources at $(20^\circ, 40^\circ)$ and $(20^\circ, 80^\circ)$. The CRMSEs values are also plotted in Figure 5(b) for the case where azimuth of one source is fixed as 40°, while that of the other source varies at a step size of 10°. The SNR in this case is fixed at $20dB$. It should be noted that the proposed SH-root-MUSIC method performs reasonably better than SH-MUSIC and SH-MVDR.

4.1.2. *Statistical Analysis*

Statistical analysis of the proposed method is presented in terms of probability of resolution for various SNRs. Two sources with DOAs $(20^\circ, 40^\circ)$ and $(20^\circ, 80^\circ)$ are considered. The confidence interval of $\zeta = 5^\circ$ was used for calculating the probability over 500 independent trials. The probability of resolution is given by

$$\begin{aligned} P_r &= \frac{1}{2T}\sum_{t=1}^{T}\sum_{l=1}^{2}[Pr(|\phi_l - \hat{\phi}_l^{(t)}| \leq \zeta)] \\ &= \frac{1}{2T}\sum_{t=1}^{T}\sum_{l=1}^{2}[sgn(\zeta - |\phi_l - \hat{\phi}_l^{(t)}|)], \end{aligned} \tag{28}$$

where $Pr(.)$ denotes the probability of an event, and $sgn(x)$ is defined as

$$sgn(x) = \begin{cases} 1 & \text{if } x \geq 0 \\ 0 & \text{if } x < 0. \end{cases} \tag{29}$$

The result is presented in Table 1 in which zero probability indicates inability of the methods to resolve sources in the given confidence interval. It is noted that the proposed method has higher probability of resolution when compared to other methods at all SNR values. It can also be concluded that a higher SNR is required for SH-MVDR to resolve co-elevated sources.

Table 1. Probability of resolution performance of various methods.

Method	**SNR (5dB)**	**SNR (10dB)**	**SNR (15dB)**	**SNR (20dB)**	**SNR (25dB)**
SH-RM	0.5131	0.7575	0.8386	0.8790	0.9032
SH-MUSIC	0	0.6198	0.8051	0.8689	0.9013
SH-MVDR	0	0	0	0.0046	0.3168

4.2. Real Data Experiments

The proposed algorithm is also verified by using real signal acquired over spherical microphone array. The experimental set-up for acquiring a source using Eigenmike® system is shown in Figure 4. A smartphone speaker is utilized as an acoustic source. The source is fixed at location $(90^\circ, 90^\circ)$ in far-field region. A narrowband signal with frequency of 1250Hz is played. The elevation of the source is assumed to be known and the azimuth is estimated using the proposed SH-root-MUSIC method.

All the $2N(= 8)$ roots within the unit circle are plotted in Figure 6. The root with argument close to 90° corresponds to the source and is represented by red star. It is noted that noisy roots are also competing in magnitude. The DOA estimation mismatch and multiple competing roots are due to the reflection of sound from the tripods, non-point sound source and microphone-source physical placement errors.

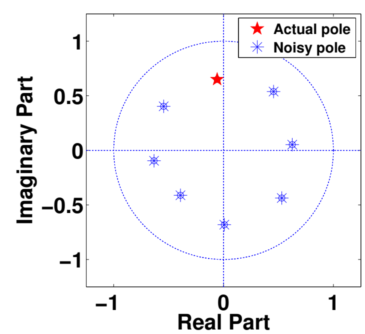

Fig. 6. Azimuth estimation of a source at $(90^\circ, 90^\circ)$ using SH-root-MUSIC. All roots within unit circle are shown for $N = 4$. The star denotes the actual estimate.

5. CONCLUSION

In this paper, theory of root-MUSIC is established in spherical harmonics domain. The theory is validated using simulation and real data experiments. The SH-root-MUSIC method does not require any search to estimate the DOAs. It provides DOA estimates as direct roots of SH-MUSIC polynomial. The Vandermonde structure of array manifold in spherical harmonics domain is shown using manifold separation technique. The robustness of the method is illustrated by using source localization experiments for various SNRs and angular separations. The RMSE and probability of resolution values indicate the relevance of the proposed method. Additionally, the method is verified with real signal acquired over spherical microphone array. Owing to its robustness and high resolution, a real time implementation for voiced-based camera steering in a meeting room can be explored.

References

[1] Arthur Barabell, "Improving the resolution performance of eigenstructure-based direction-finding algorithms," in *Acoustics, Speech, and Signal Processing, IEEE International Conference on ICASSP'83*. IEEE, 1983, vol. 8, pp. 336–339.

[2] R Roy, A Paulraj, and T Kailath, "Estimation of signal parameters via rotational invariance techniques-esprit," in *30th Annual Technical Symposium*. International Society for Optics and Photonics, 1986, pp. 94–101.

[3] Ralph O Schmidt, "Multiple emitter location and signal parameter estimation," *Antennas and Propagation, IEEE Transactions on*, vol. 34, no. 3, pp. 276–280, 1986.

[4] Harry L Van Trees, *Detection, Estimation, and Modulation Theory, Optimum Array Processing*, John Wiley & Sons, 2004.

[5] Cherian P Mathews and Michael D Zoltowski, "Eigenstructure techniques for 2-d angle estimation with uniform circular arrays," *Signal Processing, IEEE Transactions on*, vol. 42, no. 9, pp. 2395–2407, 1994.

[6] Roald Goossens, Hendrik Rogier, and Steven Werbrouck, "Uca root-music with sparse uniform circular arrays," *Signal Processing, IEEE Transactions on*, vol. 56, no. 8, pp. 4095–4099, 2008.

[7] Fabio Belloni, Andreas Richter, and Visa Koivunen, "Extension of root-music to non-ula array configurations," in *Acoustics, Speech and Signal Processing, 2006. ICASSP 2006 Proceedings. 2006 IEEE International Conference on*. IEEE, 2006, vol. 4, pp. IV–IV.

[8] Mário Costa, Andreas Richter, and Visa Koivunen, "Unified array manifold decomposition based on spherical harmonics and 2-d fourier basis," *Signal Processing, IEEE Transactions on*, vol. 58, no. 9, pp. 4634–4645, 2010.

[9] Thushara D Abhayapala and Darren B Ward, "Theory and design of high order sound field microphones using spherical microphone array," in *Acoustics, Speech, and Signal Processing (ICASSP), 2002 IEEE International Conference on*. IEEE, 2002, vol. 2, pp. II–1949.

[10] Jens Meyer and Gary Elko, "A highly scalable spherical microphone array based on an orthonormal decomposition of the soundfield," in *Acoustics, Speech, and Signal Processing (ICASSP), 2002 IEEE International Conference on*. IEEE, 2002, vol. 2, pp. II–1781.

[11] Dima Khaykin and Boaz Rafaely, "Acoustic analysis by spherical microphone array processing of room impulse responses," *The Journal of the Acoustical Society of America*, vol. 132, no. 1, pp. 261–270, 2012.

[12] Xuan Li, Shefeng Yan, Xiaochuan Ma, and Chaohuan Hou, "Spherical harmonics music versus conventional music," *Applied Acoustics*, vol. 72, no. 9, pp. 646–652, 2011.

[13] Lalan Kumar, Ardhendu Tripathy, and Rajesh M Hegde, "Robust multi-source localization over planar arrays using music-group delay spectrum," *Signal Processing, IEEE Transactions on*, vol. 62, no. 17, pp. 4627–4636, Sept 2014.

[14] Lalan Kumar, Kushagra Singhal, and Rajesh M Hegde, "Robust source localization and tracking using music-group delay spectrum over spherical arrays," in *Computational Advances in Multi-Sensor Adaptive Processing (CAMSAP), 2013 IEEE 5th International Workshop on*, Dec 2013, pp. 304–307.

[15] Lalan Kumar, Kushagra Singhal, and Rajesh M Hegde, "Near-field source localization using spherical microphone array," in *Hands-free Speech Communication and Microphone Arrays (HSCMA), 2014 4th Joint Workshop on*, May 2014, pp. 82–86.

[16] Arun Parthasarathy, Saurabh Kataria, Lalan Kumar, and Rajesh M. Hegde, "Representation and modeling of spherical harmonics manifold for source localization," in *Acoustics, Speech and Signal Processing (ICASSP), 2015 IEEE International Conference on*, April 2015, pp. 26–30.

[17] Boaz Rafaely, "Plane-wave decomposition of the sound field on a sphere by spherical convolution," *The Journal of the Acoustical Society of America*, vol. 116, no. 4, pp. 2149–2157, 2004.

[18] Earl G Williams, *Fourier acoustics: sound radiation and nearfield acoustical holography*, Access Online via Elsevier, 1999.

[19] John McDonough, Kenichi Kumatani, Takayuki Arakawa, Kazumasa Yamamoto, and Bhiksha Raj, "Speaker tracking with spherical microphone arrays," in *Acoustics, Speech and Signal Processing (ICASSP), 2013 IEEE International Conference on*. IEEE, 2013, pp. 3981–3985.

[20] James R Driscoll and Dennis M Healy, "Computing Fourier transforms and convolutions on the 2-sphere," *Advances in applied mathematics*, vol. 15, no. 2, pp. 202–250, 1994.

[21] Boaz Rafaely, "Analysis and design of spherical microphone arrays," *Speech and Audio Processing, IEEE Transactions on*, vol. 13, no. 1, pp. 135–143, 2005.

[22] *The Eigenmike Microphone Array*, http://www.mhacoustics.com/.